Electronic Supplementary Material (ESI) for Physical Chemistry Chemical Physics.

Electronic Supplementary Information (ESI)

Why Ice-Binding Type I Antifreeze Protein Acts as a Gas Hydrate Crystal Inhibitor

S. Alireza Bagherzadeh,[a] Saman Alavi,[a,b*] John A. Ripmeester,[a,b*] and Peter Englezos[a*]

[a] Department of Chemical and Biological Engineering, The University of British Columbia, 2360 East Mall, Vancouver BC, Canada V6T1Z3.

[b] National Research Council of Canada, 100 Sussex Dr., Ottawa ON, Canada K1A0R6.

[*] Correspondence should be addressed to: Email: saman.alavi@nrc-cnrc.gc.ca; Email: john.ripmeester@nrc-cnrc.gc.ca; Email: peter.englezos@ubc.ca, Tel: +1 (604)822-6184, Fax: +1 (604)822-6003.

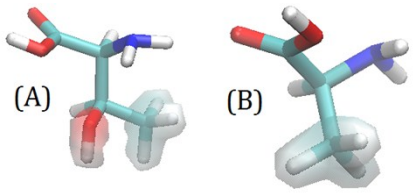

Fig. S1. Chemical structures of (A) the THR residue and (B) the ALA residue. The side chains are emphasized by transparent volumes around them. THR has one hydroxyl and one methyl side chain whereas ALA only has one methyl side chain. Color scheme: carbon, cyan; oxygen, red; hydrogen, white; nitrogen: blue.

AFP/Water simulation

The initial and final configurations for the AFP/Water simulation are given in Fig. S2(A) and (B). It is evident that the *wf*-AFP remains stable under the function of the amber99sb-ildn force field at simulation conditions of 275 K and 800 bar. The radial distribution function (RDF) of water oxygen (OW) around hydroxyl oxygen (OG1) and methyl carbon (CG2) of THR residues during the AFP/Water simulation are plotted in Fig. S2(C). The first peak for the OW-OG1 RDF occurs at 0.282 nm and the first minimum is at 0.356 nm which is indicative of hydrogen bonding between the hydroxyl group of the THR residue and water molecules. The first peak for the OW-CG2 RDF occurs at a larger distance, 0.37 nm, which is expected, due to the hydrophobicity of the methyl group. For reference, the radial dimensions from the center of the elliptical structure I hydrate large cages are 0.306 and 0.254 nm. Water structuring around the hydrophobic methyl group is more pronounced and the OW-CG2 RDF shows a clear second peak at 0.632 nm. However, this is not evident in the OW-OG1 profile which does not show evidence of water structuring at intermediate distances. The influence of hydrophobic solutes on local water order is a well-known phenomenon.[S1]

Root Mean Square Deviation (RMSD) of the backbone of the protein is plotted in Fig. S3. It initially increases and after ~0.3 ns, gradually levels off at about 0.2 nm, suggesting that there is no substantial change in protein structure at the conditions of simulation (275 K and 800 bar). The average length and radius of the helix during 5 ns of simulation are 4.77 nm and 0.242 nm, respectively. Furthermore, average Φ and Ψ, the Ramachandran dihedral angles[S2] for rotation around the bond between N-Cα and Cα-C, respectively, are -67.2° and -37.5° which are within the range for α-helical structure (Φ=-60±10 and Ψ=-45±10).

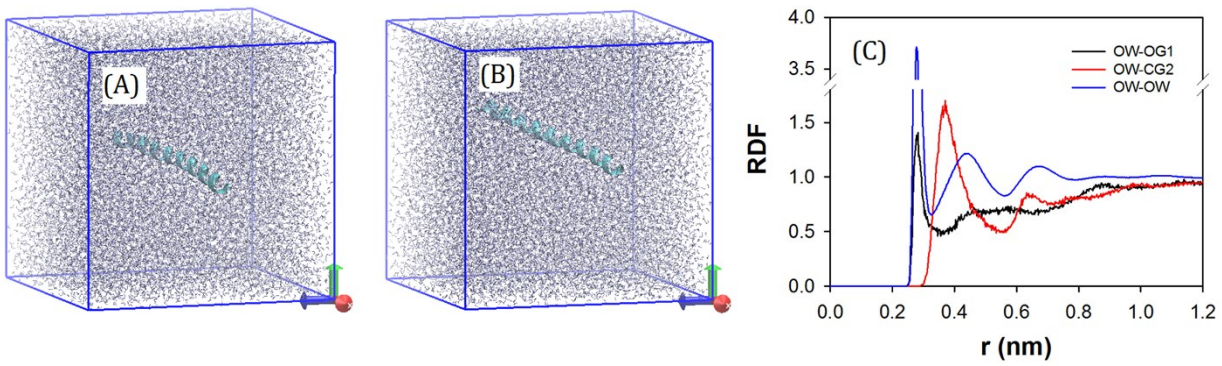

Fig. S2. (A) Initial (0ns) and (B) final (5 ns) configurations of the AFP/Water simulation. α–helical structure of *wf*-AFP is evident in the middle of the simulation box. The size of the cubic box is 8.421 nm and blue lines represent water molecules. *x*, *y* and *z* axes are colored as red, green and blue, respectively. (C) Radial distribution functions for water oxygen with the THR hydroxyl oxygen (OW-OG1, black), the THR terminal methyl carbon (OW-CG2, red) and other water oxygens (OW-OW, blue). The first peak of the OW-OG1 RDF occurs at 0.282 nm, similar to the OW-OW first peak, while the first peak of OW-CG2 occurs at 0.37 nm due to hydrophobic characteristics of THR methyl group.

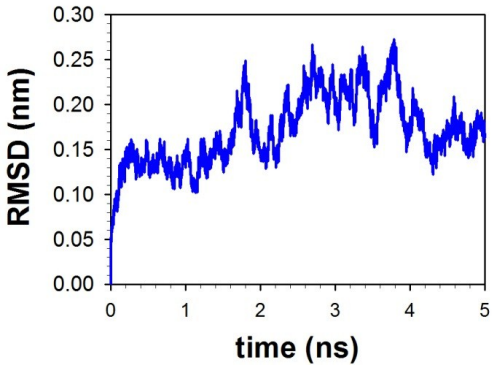

Fig. S3. Root mean square deviation of the backbone of the protein during the AFP/Water simulation. RMSD remains below 0.3 nm suggesting no significant change in the α-helical structure of *wf*-AFP under simulation conditions of 275 K and 800 bar.

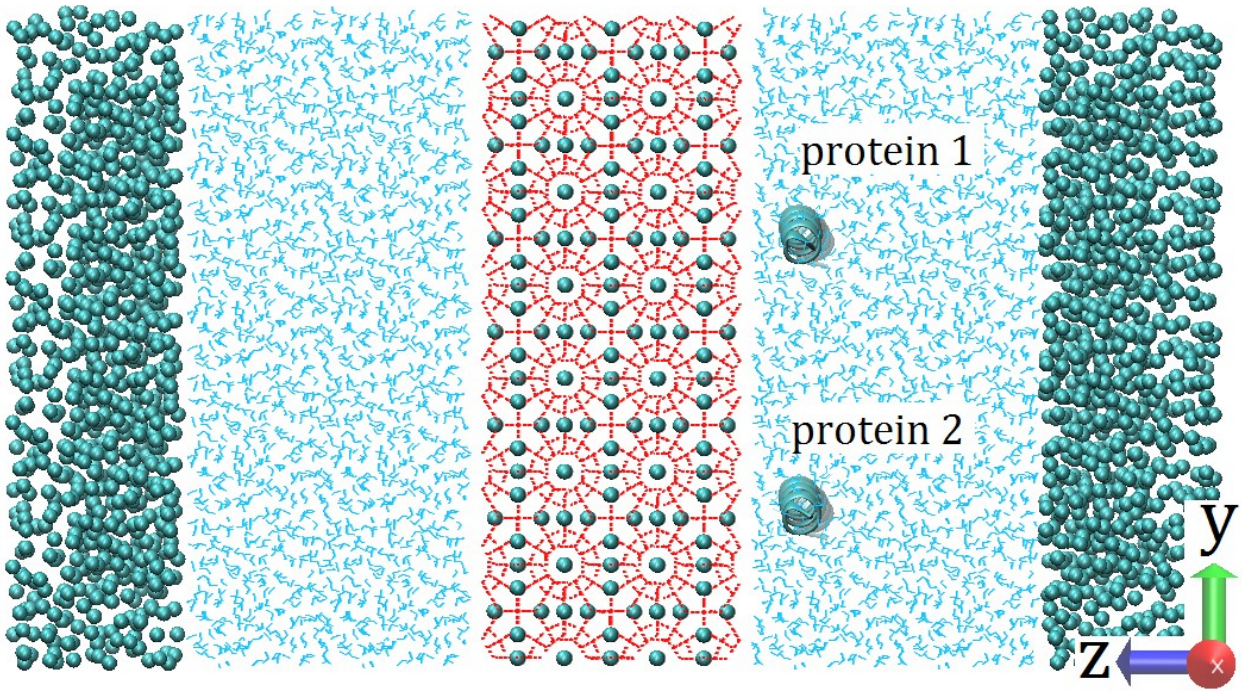

Fig. S4. *yz*-projection of the initial configuration of the *case II* simulation. The AFP is aligned with the long axis along the *x*-direction. Simulation box sizes along the *x*, *y* and *z*-directions are 8.421, 8.421 and 15.639 nm. *wf*-AFP, methane in the gas phase and water in the liquid phase are represented by a cyan ribbon, cyan spheres and blue lines, respectively. Hydrate water and methane are shown as red hydrogen bonds and cyan spheres in the middle of the box, respectively.

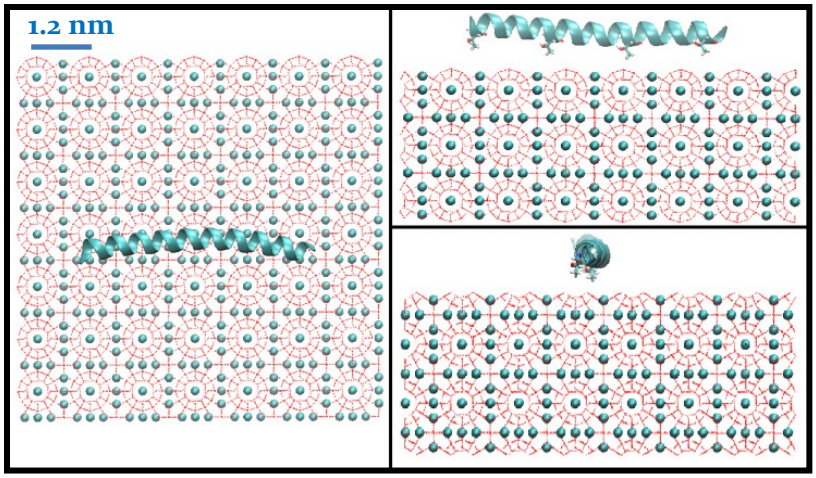

Fig. S5. Relative position of *wf*-AFP with respect to the hydrate block in *case I* simulation. The protein is roughly 1 nm away from the hydrate surface. Same relative distance is used for the *case II* simulation. The cyan helix represents the *wf*-AFP. For clarity only threonine residue side chains are shown. Liquid water molecules and gas phase methane are not shown. Hydrate methane and water molecules are represented by cyan spheres and red lines (H-bonds), respectively. Left pane: *xy* view; Top right: *xz* view; Bottom right: *yz* view.

Table S1. Number of molecules present in each simulation set.

Simulation set [total time]	AFP/Water [5 ns]	AFP/Hydrate/Water/Gas	
		Case I [200 ns]	Case II [100 ns]
Protein (wf-AFP)	1	1	2
Water (liquid)	19669	16552	16762
Water (hydrate)	-	6468	6468
Methane (hydrate)	-	1029	1029
Methane (gas)	-	2879	3011

Protein bending during the *case I* simulation

Figure S6(A) illustrates snapshots of the protein structure at different times. It is evident that the tail segment of the protein near the water/gas interface has denatured and lost its helical structure. More importantly one can see that although between 120 and 140 ns a substantial portion of the protein has unfolded, it refolds to its helical structure afterwards. Nevertheless, the section of the AFP which is immersed in the liquid water phase, especially the part near the hydrate block, retains its helical structure for the duration of the simulation.

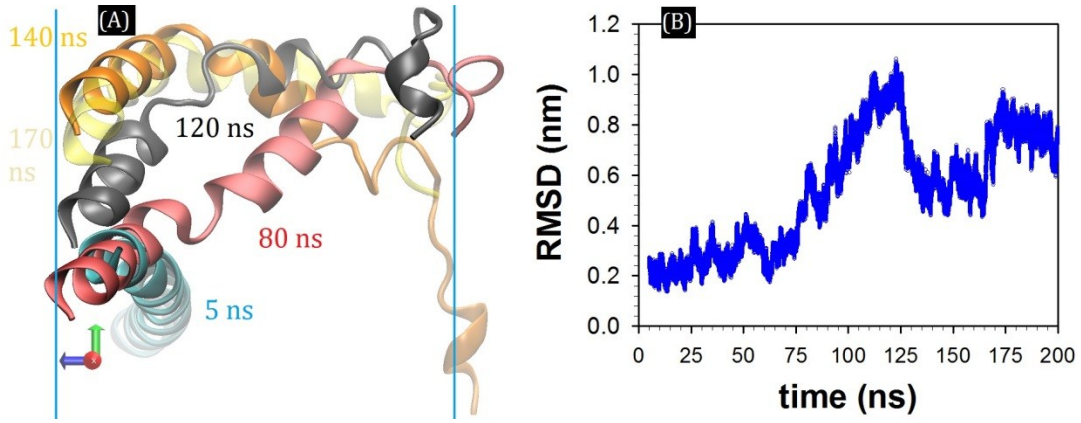

Fig. S6. (A) The structure of *wf*-AFP at different times during the case I simulation. Cyan, red, black, orange and transparent yellow correspond to 5, 80, 120, 140 and 170 ns, respectively. The blue line on the left shows the approximate position of the hydrate/water interface while the one on the right shows that of the water/gas interface. Other molecules are not shown for clarity. (B) RMSD of the *wf*-AFP during the *case I* simulation. There is a significant change in the backbone structure of the protein after 60 ns. This substantial structural change can be seen as unfolding of the section of the protein which is not adjacent to the water/hydrate interface.

The protein begins to bend near the ALA 14 site at 53.9 ns due to thermal fluctuations. This bend occurs long before the other end of the protein reaches the gas/water interface at 71.1

ns. The thickness of liquid water layer plays a role in the observation of this behavior and the bending of the protein in systems with larger thickness of liquid water layer will be investigated in future simulations. Figure S6(B) shows the RMSD of the backbone of the *wf*-APF for *case I* during the 200 ns of the simulation. The RMSD slowly increases until about 60 ns, after which substantial structural deformation occurs leading to RMSD values as high as 1 nm. This significant structural change is attributed to the end of protein diffusing into the gas/water interface.

Table S2. Atoms of the side chain of all residues of wf-AFP around which the F_3 is calculated.

Residue	Side chain	Atom	Residue	Side chain	Atom
1ASP	carboxyl	OD1	20ALA	methyl	CB
		OD2	21ALA	methyl	CB
2THR	methyl	CG2	22GLU	carboxyl	OE1
	hydroxyl	OG1			OE2
3ALA	methyl	CB	23LEU	methyl	CD1
4SER	hydroxyl	OG		methyl	CD2
5ASP	carboxyl	OD1	24THR	methyl	CG2
		OD2		hydroxyl	OG1
6ALA	methyl	CB	25ALA	methyl	CB
7ALA	methyl	CB	26ALA	methyl	CB
8ALA	methyl	CB	27ASN	carbonyl	OD1
9ALA	methyl	CB		amine	ND2
10ALA	methyl	CB	28ALA	methyl	CB
11ALA	methyl	CB	29ALA	methyl	CB
12LEU	methyl	CD1	30ALA	methyl	CB
		CD2	31ALA	methyl	CB
13THR	methyl	CG2	32ALA	methyl	CB
	hydroxyl	OG1	33ALA	methyl	CB
14ALA	methyl	CB	34ALA	methyl	CB
15ALA	methyl	CB	35THR	methyl	CG2
16ASN	carbonyl	OD1		hydroxyl	OG1
	amine	ND2	36ALA	methyl	CB
17ALA	methyl	CB	37ARG	amine	NH1
18LYS	ammonium	NZ			NH2
19ALA	methyl	CB			

References

S1. N. Galamba, Water Tetrahedrons, Hydrogen-Bond Dynamics, and the Orientational Mobility of Water around Hydrophobic Solutes. *J. Phys. Chem. B*, 2014, **118,** 4169–4176.

S2. G. N. Ramachandran, C. Ramakrishnan and V. Sasisekharan, Stereochemistry of polypeptide chain configurations. *J. Mol. Biol.*, 1963, **7,** 95–99.